ORIGINAL ARTICLE

Prediction method of surface residual subsidence for land resource reuse after low-carbon underground coal gasification

Chao Tang[1] · Huaizhan Li[1] · Guangli Guo[1] · Fu Chen[1] · Wei Li[1] · Yafei Yuan[1] · Guangli Dai[2] · Wenqi Huo[1] · Jianfeng Zha[1] · Xuewei Zhang[1] · Chao Liu[2] · Huaan Zhou[1]

Abstract
Underground coal gasification (UCG) is an important part of the low-carbon green coal mining technology system. With the implementation of the carbon peaking and carbon neutralization and the maturity of UCG, UCG will inevitably perform large-scale and industrialized production, which will certainly cause some issues such as serious waste of UCG sites caused by large-scale surface residual subsidence and poor foundation of fractured rocks. The key to the reuse of the surface site after UCG is to ensure that the surface residual subsidence does not exceed the design index of the building (structure). However, there is still a lack of methods for predicting residual subsidence on the surface of UCG. Under such background, combined with the characteristics of the UCG process, this paper analyzed the mechanism of the surface residual subsidence after UCG, and concluded that the root resource of the surface residual subsidence after UCG was the stripping and yielding of the hyperbolic coal pillars. Next, a calculation model of the maximum stripping width and yielding zone width of the "hyperbolic" coal pillar for UCG was established by the theoretical analysis method, and a method for predicting the surface residual subsidence with the consideration of coal pillar stripping and yielding was proposed and applied to Ulanqab UCG test site. The research findings have important theoretical and practical significance for the UCG site stability evaluation and land resource reuse.

Keywords Underground coal gasification · Surface residual subsidence · Maximum stripping width · Yielding zone width · Prediction method

Introduction

With the advancement of global "carbon peaking" carbon neutral'(Hargroves et al. 2016; Le Quéré et al. 2015; Qin et al. 2021; Sovacool 2022), the energy structure is being adjusted in the direction to low-carbon and non-carbonization(Johnstone et al. 2021; Slamersak et al. 2022; Suzuki et al. 2016; Wu et al. 2018). As a significant part of the energy structure, how to use coal resources in a low-carbon, green and clean has become a research hotspot. Underground coal gasification (UCG), a revolutionary technology,

may radically transform the traditional coal industry into a clean and environmentally friendly energy industry (Al-Ghussain 2019; Bhutto et al. 2013; Prabu 2015; Xie et al. 2020). In the past decade, the progress of UCG has been increasing and the existing UCG process has been able to meet the requirements of industrialization and large-scale production (Ariyoshi et al. 2016; Friedmann et al. 2008; Walker 2014).

Nevertheless, with the industrialization and large-scale production of UCG, the issues including large-scale surface subsidence and fractured rocks will inevitably occur, which will restrict the reuse of UCG sites and cause serious waste of UCG surface sites. The key to the reuse of UCG sites is to assess the stability of gasification sites (Li et al. 2019; Luan et al. 2020). If the gasification area is evaluated as stable, ground buildings can be constructed. While the gasification area is unstable, the gasification site requires to be regulated. The core of the stability evaluation of the UCG site is to calculate its residual subsidence deformation. By comparing

✉ Huaizhan Li
lihuaizhan@cumt.edu.cn

1 School of Environment and Spatial Informatics, China University of Mining and Technology, Xuzhou 221116, China

2 Fifth Geological Brigade, Geology and Mineral Resources Bureau of Jiangsu, Xuzhou 221116, China

the difference between the residual surface deformation and the evaluation index, it can be determined whether the gasification area site is stable.

However, there is currently no method for predicting the UCG surface residual subsidence, leading to a lack of the scientific basis to evaluate the stability of the gasification area. Nonetheless, some scholars have studied research on the prediction method of residual subsidence in well mining. For example, Salamon and Merwe (Salamon and Madden 1998; Van der Merwe 2003; van der Merwe and Mathey 2013) found that the room-type pillar will suffer progressive instability, causing secondary deformation of the surface. Yu Yang et al. (Yang et al. 2017) deduced a computational method of maximum stripping width for strip mining. Changfu Huang et al. (Huang et al. 2020) explored the residual subsidence in goaf of steeply inclined extra-thick coal seam and established a residual subsidence dynamic prediction function. Guo Guangli et al. (Guang-li et al. 2002) established a stochastic medium model for predicting the residual subsidence of the surface above the deep longwall goaf. Guo Qingbiao et al. (Guo et al. 2021) employed the probability integral method to establish a prediction model of surface residual subsidence by analyzing the spatial distribution and shape characteristics of voids. Ximin Cui et al. (Cui et al. 2020) proposed a model for calculating the subsidence coefficient of surface residual deformation and quantified the annual residual subsidence, cumulative residual subsidence and future potential cumulative residual subsidence under given geological mining conditions. Meinan Zheng and Donghui Chen (Chen et al. 2020; Zheng et al. 2018) applied the InSAR technology to study the post-mining subsidence. DENG Ka-zhong et al. (Ka-zhong et al. 2012) built the calculating method of residual deformation coefficient of old goaf areas in shallow long walls under

the building load action. The research results of the above-mentioned surface residual subsidence prediction method for the well-working mining surface provide an important reference for the construction of the surface residual subsidence model of UCG.

Based on this, this paper combines the UCG process and the geological and mining conditions of the gasification test area and applies the theoretical analysis method to reveal the mechanism of the surface residual subsidence of UCG. Besides, a calculating model of maximum stripping and yielding zone width of "hyperbolic" coal pillar is established and a surface residual subsidence predicting method of UCG considering the coal pillar stripping and yielding is proposed. The research outcomes have a significant theoretical and practical meaning for the stability evaluation of the UCG sites and the reuse of the land resources after UCG.

Overview of underground coal gasification process

The internationally advanced "Strip mining-regional mining" gasifier backward controlled gas injection underground gasification process is located in Ulanqab, China, and four gasification working faces are separated. As shown in Fig. 1, directional drilling and combustion are used to form the gas outlet and ignition column, and drill holes are drilled in the middle of the coal seam by directional drilling to ignite at the starting point of gasification. Next, the backward control of coal seam gasification is adopted until the first working face is gasified, and the gasification operations of the second, third and fourth gasification working faces are, respectively, completed by the above method. The specific gasification process is as follows:

Fig. 1 Schematic diagram of the "Strip mining-regional mining" gasifier backward controlled gas injection underground gasification technology
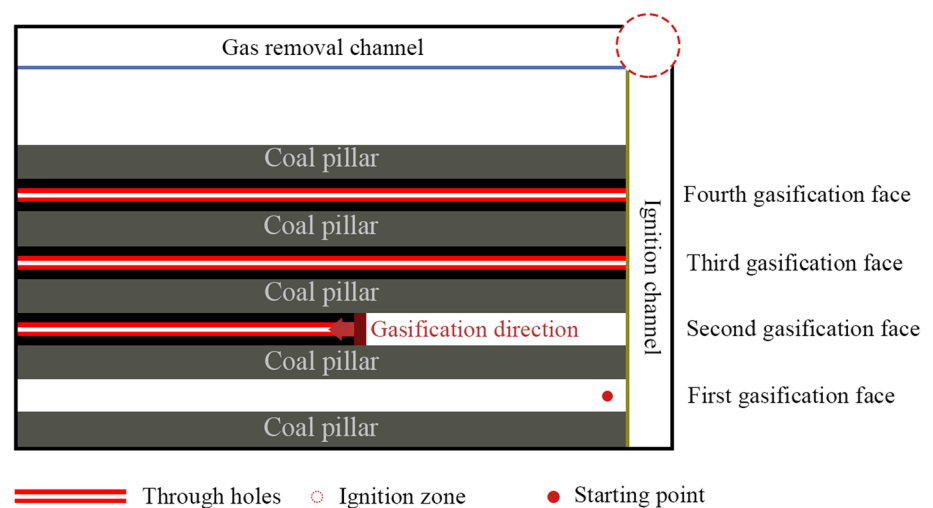
(1) The ignition area was ignited, and it took 60 days to form a gas removal channel with a length of 170m long and a width of 5m.

(2) The ignition channel processing took 60 days.

(3) UCG was carried out on the first gasification face starting from the ignition channel and ending at the end of the face, which took 90 days and formed a combustion space area with a length of 170m and a width of 16m.

(4) After the completion of the first gasification face, the UCG operation of the second gasification face will be conducted. It will take 90 days from the ignition channel to the end of the working face, forming a gasification and combustion space area with a length of 170m in length and a width of 5m.

(5) After the second gasification face was completed, the UCG of the third gasification face was performed, starting from the ignition channel and ending at the end of the face, which lasted for 90 days and formed a combustion space area with a length of 170m and a width of 16m.

(6) The gasification operation of the fourth gasification working face was carried out, starting from the ignition channel and ending at the end of the face, which took 90 days and formed a combustion space area with a length of 170m and a width of 16m.

(7) End the gasification operation and perform furnace shutdown operation.

Combined with the above-mentioned characteristics of the UCG process, the combustion space area gradually spread from the through holes to the surrounding, forming a "ring runway-like" pattern, while the isolated coal pillar in the middle of the gasifier is "hyperbolic" (Li et al. 2017). The shape of the isolated coal pillar and the gasifier after "Strip mining-regional mining" gasifier backward controlled gas injection underground gasification is shown in Fig. 2.

Mechanism analysis of surface residual subsidence of UCG

After UCG, surface subsidence occurred and overlying strata were gradually stable after a long time of compaction. However, there still exist phenomena such as insufficient compaction of the falling zone and boundary voids on both sides of the combustion space area. With the decrease of the coal pillar support force and the external additional loads, the overlying rock secondary equilibrium structure will be broken, the combustion space area will awake and surface subsidence will appear. The mechanism of surface residual subsidence after UCG is as follows:

(1) When the overlying strata are stable, the unbroken part of the rock formation or the part that does not produce severe deformation, or the part of the stratum that has been broken but can still be neatly arranged, can form arch or beam structure to support the rock above and transfer the overburden pressure to coal pillar on both sides. If the structure is unstable, the overlying strata can move and deform again, and further develop upward to the ground surface, resulting in surface residual subsidence.

(2) Under the sustained action of groundwater, efflorescence, and overburden pressure, the inter-grain connection of the coal pillar is destroyed, which reduces the strength of the coal pillar on both sides of the combustion space area. The phenomenon of peeling and yielding appeared on both sides of the "hyperbolic" coal pillar. Thus, the stress area of the coal pillar is continuously fed from both sides to the center, resulting in changes at both ends of the arch or beam, which will increase the movement and deformation of the surface above the combustion space area to a certain extent.

Fig. 2 Morphology of combustion space area after "Strip mining-regional mining" gasifier backward controlled gas injection underground gasification
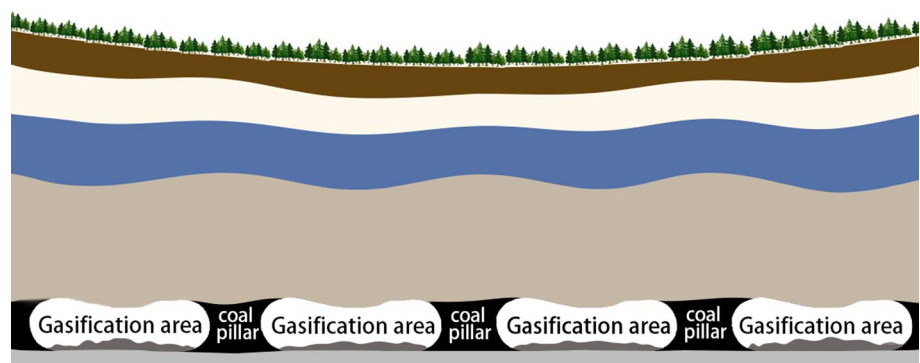
(3) The overburden pressure will directly act on the broken rock and gasification residue in the combustion space area. Although the overlying strata trends to be in a stable state, the structural plane of the rock blocks and ash is further compressed and deformed by closure and slippage due to the action of the upper additional load on the upper part. The fractures between the rock blocks, ash, and rock and ash are further compressed. This action is transferred to the surface, causing surface residual subsidence, but the amount of deformation is very limited.

(4) Under the support of the arch structure, under-compact areas and residential cavities will appear on both sides of the combustion space area. Under the action of overburden pressure, the under-compact area will be further compressed, and some rock blocks in the under-compact area will be squeezed into the boundary voids. Besides, coal blocks stripped from coal pillars will be scattered into the boundary voids and the overlying strata above the boundary voids will collapse and compact, all of which will cause residual subsidence of surface.

In general, the main reason for the surface residual subsidence of UCG is the stripping and yield softening of the "hyperbolic" coal pillar under the action of the long-term groundwater, efflorescence, overburden pressure, and other factors, as shown in Fig. 3.

Calculation method for maximum stripping width and yielding zone width of "Hyperbolic" coal pillar in UCG

Combined with the above-described mechanism of surface residual subsidence of UCG, it can be concluded that the surface residual subsidence is mainly due to the stripping and yielding of coal pillar on both sides of the combustion space area, leading to the increase of the skewback and arch height of the overburden stress balance and causes the surface "secondary" deformation. Therefore, to calculate the surface residual subsidence of UCG, we should calculate the stripping and yielding zone width of the "hyperbolic" coal pillar first. Hence, this section mainly adopts the theoretical analysis method to establish the maximum stripping and yield zone width calculation model of the "hyperbolic" coal pillar of UCG.

Computation approach for maximum stripping width of coal pillar

When the "hyperbolic" coal pillar is subjected to the overburden stress, the stress concentration occurs in the upper curved part of the edge, which is more prone to peeling. On the other hand, the lower bending part is under less pressure and has coal ash to provide lateral pressure, and the degree of peeling

Fig. 3 Mechanism diagram of surface residual subsidence of UCG
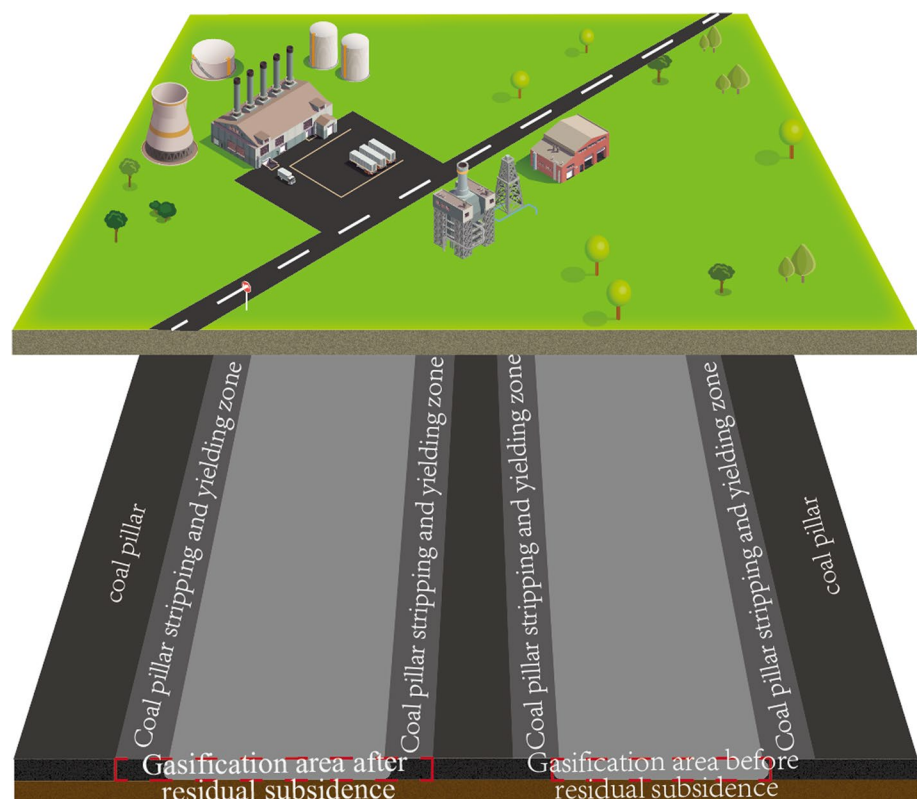
is relatively small. The stripped coal block is regarded as a granular medium, and the stripped coal block continuously accumulates in the combustion space area (Yu et al. 2018). Without considering that the pressure on the coal pillar edge decreases gradually from top to bottom, so it is assumed that the coal pillar edge is elliptical after stripping.

The sketch map of the shape of "hyperbolic" coal pillar stripping after UCG is shown in Fig. 4. Assuming that the width of the coal pillar before stripping is T, m; the arch height is a, m; the stripping width at the top of the coal pillar is d, m; the height of the coal pillar is m, m; the ash height is h', m; when the coal pillar stops stripping, the angle between the stacked coal blocks and the horizontal surface is the rest angle, symbolized as θ, (°); the maximum stripping width of the coal pillar is taken as the middle part, defined as b, m. L is the maximum length of coal pillar, m.

It can be seen from Fig. 3 that

$$L = T + 2a. \tag{1}$$

According to the equivalent mining thickness, the ash formation rate after coal combustion is set as k_p. If the ash has been compacted, the real mining height can be written as H':

$$H' = m - k_p m. \tag{2}$$

If the coal pillar center is taken as the origin, the horizontal direction is the x-axis, the vertical direction is the y-axis to establish a coordinate system. The boundary of "hyperbola" of the coal pillar must pass through the points $(\frac{L}{2} - a, 0)$ and $(\frac{L}{2}, \frac{m}{2})$, and the hyperbolic equation can be solved according as

$$\frac{x^2}{u^2} - \frac{y^2}{v^2} = 1 \tag{3}$$

where $u^2 = \left(\frac{L}{2} - a\right)^2$, $v^2 = \dfrac{m^2}{4\left[\frac{L^2}{4(\frac{L}{2}-a)^2} - 1\right]}$.

After the coal pillar is peeled off, the boundary ellipse takes the intersection of the original coal pillar edge and the roof plate as the center of the circle. The maximum stripping width

and the height of the coal pillar are, respectively, set as the long axis and the short axis, and the equation is

$$\frac{\left(x - \frac{L}{2}\right)^2}{d^2} + \frac{\left(y - \frac{m}{2}\right)^2}{m^2} = 1. \tag{4}$$

Although the lower part of the coal pillar is stripped off by the lateral pressure of ash, expansion capacity is small, and its hulking coefficient is considered to be 1. The volume of stripped coal blocks is

$$V_p = k\left(\frac{\pi m d}{4} - V_s - V_t\right) + V_s \tag{5}$$

$$V_p = \frac{H'^2}{2\tan\theta} + dh' - dm + \frac{\pi m d}{4} - V_r \tag{6}$$

where k is the hulking coefficient of the stripped coal blocks:

$$V_t = 2\int_{\frac{L}{2}-a}^{\frac{L}{2}}\left(v\sqrt{\frac{x^2}{u^2} - 1}\right)dx \tag{7}$$

$$V_r = \int_u^{\frac{L}{2}\sqrt{1+\left(\frac{m}{2}-h'\right)^2}}\left[-\left(\frac{m}{2} - h'\right) + v\sqrt{\frac{x^2}{u^2} - 1}\right]dx \tag{8}$$

$$V_s = \int_{-d\sqrt{1-\left(\frac{-m+h'}{m}\right)^2}+\frac{L}{2}}^{\frac{L}{2}}\left[-\left(\frac{m}{2} - h'\right) + m\sqrt{1 - \left(\frac{x - \frac{L}{2}}{d}\right)^2} + \frac{m}{2}\right]$$
$$dx - V_r \tag{9}$$

V_r, V_s, V_t are the areas of the regions shown in Fig. 5. Combining the above equations yields:

$$d = \frac{V_s + V_r - k(V_t + V_s) - \frac{(H')^2}{2\tan\theta}}{h' - m + \frac{\pi m}{4} - \frac{k\pi m}{4}} \tag{10}$$
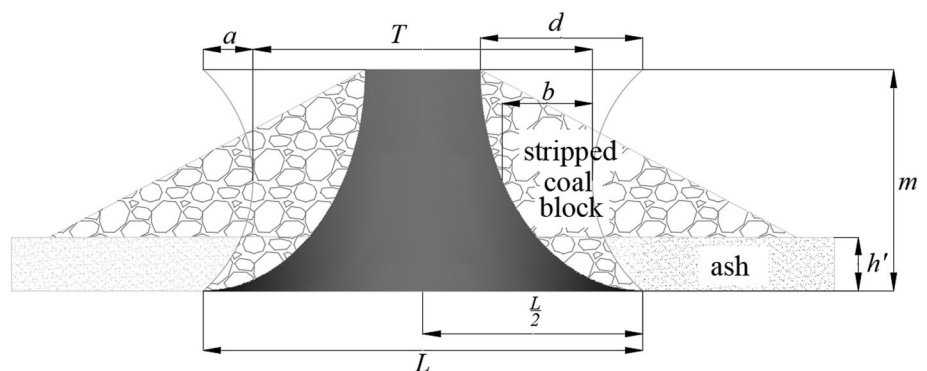
Fig. 4 Coal pillar stripping model

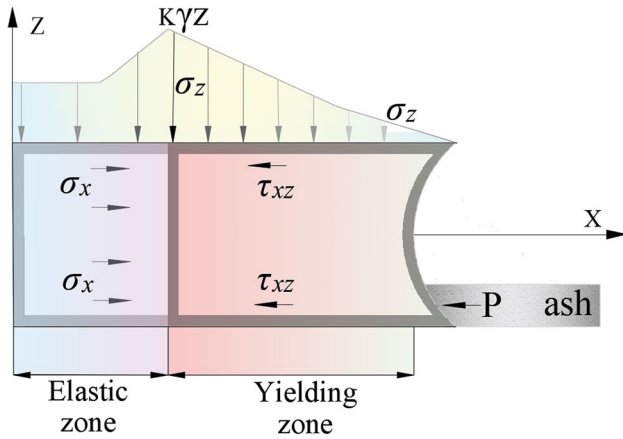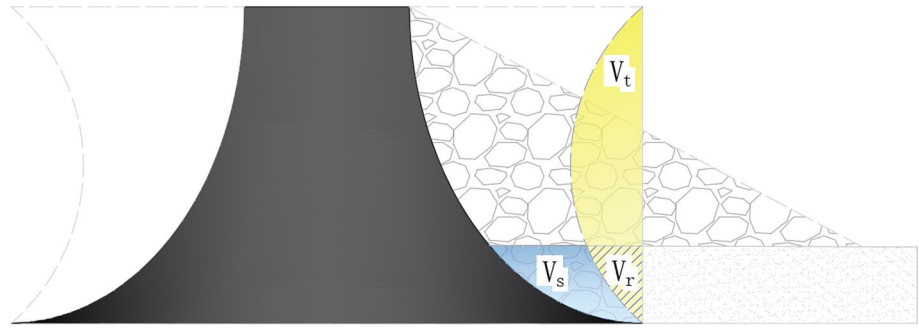**Fig. 5** Coal pillar calculation partition

Fig. 6 Coal pillar mechanical model after UCG

$$b = \frac{T}{2} - \left(-d\sqrt{\frac{3}{4}} + \frac{L}{2}\right) = \frac{V_s + V_r - k(V_t + V_s) - \frac{(H')^2}{2\tan\theta}}{h' - m + \frac{\pi m}{4} - \frac{k\pi m}{4}}\sqrt{\frac{3}{4}} - a.$$ (11)

Calculation method of yield zone width of coal pillar

Considering the geometric characteristics and forces of the coal pillar without shaft-type UCG, to apply the Coulomb criterion to simplify and derive the yield zone width of the coal pillar from an ideal angle. The calculation model of the yield zone width of the coal pillar is simplified as a plane problem perpendicular to the gasification direction. Meanwhile, the coal pillar is regarded as a uniform, continuous and isotropic ideal elastic–plastic material. The plane is symmetrical, and the mechanical model is shown in Fig. 6.

From the Mohr–Coulomb strength criterion, it follows a cut plane, such that:

$$\tau_{zx} = -(C + \sigma_z \tan\varphi)$$ (12)

where τ_{zx} is the shear stress at the coal seam interface(kpa), pointing in the negative direction of x, C is the cohesive force between the coal seam and the top and bottom plates(kpa),

σ_z is the vertical stress above the coal pillar (kpa), and φ is the internal friction angle between the coal seam and the top and bottom layers(°).When $x = x_0$, it has:

$$[\sigma_z]_{x=x_0} = K\gamma Z, \ \sigma_x = A[\sigma_z]_{x=x_0}$$ (13)

where K is the stress concentration coefficient of the coal pillar, γZ is the original rock stress (kPa), and A is the lateral pressure coefficient between the elastic zone and the plastic zone.

The contact surface between the coal pillar and the ash is a curved surface, and the contact surface is regarded as a slope to simplify the calculation. The horizontal passive earth pressure on the coal pillar is (Jian et al. 2009)

$$P = -\frac{\gamma' h'^2}{2w}$$ (14)

where h' is the height of ash, and γ' is the average gravity density of ash:

$$w = \frac{\tan\delta - \tan\alpha}{\tan\alpha + \cot\theta'} + \frac{(\tan\phi - \cot\theta')(1 + \tan\delta\tan\alpha)}{(\tan\phi + \cot\theta')(1 + \tan\delta\tan\alpha)}$$ (15)

where θ' is the inclination angle of the most dangerous sliding surface, α is the angle between coal pillar and vertical plane, δ is the coal pillar and ash friction angle, and ϕ is the internal friction angle of ash.

Ignoring the volume force, the basic equation of the mechanical model is

$$\begin{cases} \dfrac{\partial\sigma_z}{\partial z} + \dfrac{\partial\tau_{xz}}{\partial x} = 0 \\ \dfrac{\partial\sigma_x}{\partial x} + \dfrac{\partial\tau_{xz}}{\partial z} = 0 \\ \tau_{zx} = -(C + \sigma_z\tan\varphi) \end{cases}$$ (16)

Inserting Eq. (12) into Eq. (16), the basic equation of the mechanical model becomes:

$$-\frac{\partial\sigma_z}{\partial x}\tan\varphi + \frac{\partial\sigma_z}{\partial z} = 0.$$ (17)

From the mathematical equation, we can set:

$$\sigma_z = f(x)g(z) + B_1. \tag{18}$$

Inserting Eq. (18) into Eq. (17):

$$-f'(x)g(z)\tan\varphi + f(x)g'(z) = 0. \tag{19}$$

After the simplification, it can attain that:

$$\frac{f'(x)}{f(x)}\tan\varphi = \frac{g'(z)}{g(z)}. \tag{20}$$

There exists a constant B, such that

$$\begin{cases} \dfrac{f'(x)}{f(x)}\tan\varphi = B \\ \dfrac{g'(z)}{g(z)} = B \end{cases}. \tag{21}$$

Solving for the original function gives

$$\begin{cases} f(x) = B_1' e^{\frac{B}{\tan\varphi}x} \\ g(z) = B_2' e^{Bz} \end{cases}. \tag{22}$$

Therefore

$$\sigma_z = B_1' B_2' e^{\frac{B}{\tan\varphi}x} e^{Bz} + B_1 \tag{23}$$

$$\tau_{xz} = -[(B_1' B_2' e^{Bz} e^{\frac{Bx}{\tan\varphi}} + B_1)\tan\varphi + C]. \tag{24}$$

By substituting the parameter $z = \frac{m}{2}$ into Eq. (24), it can be deduced that:

$$B_0 = B_1' B_2' e^{\frac{Bm}{2}}. \tag{25}$$

Therefore

$$\begin{cases} \sigma_z = B_0 e^{\frac{Bx}{\tan\varphi}} + B_1 \\ \tau_{xz} = -[(B_0 e^{\frac{Bx}{\tan\varphi}} + B_1)\tan\varphi + C] \end{cases}. \tag{26}$$

Considering the coal pillar to be continuous and in an equilibrium state, according to the equilibrium differential equations, Eq. (27) can be derived:

$$mA[\sigma_z]_{x=x_0} + 2\int_0^{x_0}[\tau_{xz}]dx - P = 0. \tag{27}$$

The derivative of the above equation yields:

$$mA\frac{d[\sigma_z]_{x=x_0}}{dx_0} + 2[\tau_{xz}]_{x=x_0} = 0. \tag{28}$$

Inserting Eq. (12)

$$mA\frac{d[\sigma_z]_{x=x_0}}{dx_0} - 2\tan\varphi[\sigma_z]_{x=x_0} - 2C = 0. \tag{29}$$

The solution is

$$[\sigma_z]_{x=x_0} = B' e^{\frac{2\tan\varphi}{mA}x_0} - \frac{C}{\tan\varphi}. \tag{30}$$

In the formula

$$\begin{cases} B = \dfrac{2\tan^2\varphi}{mA} \\ B_1 = -\dfrac{C}{\tan\varphi} \\ B_0 = B' \end{cases}. \tag{31}$$

Inserting Eq. (31) into Eqs. (26) and (27):

$$\begin{cases} B_0 e^{\frac{2\tan\varphi}{mA}x_0} - \dfrac{C}{\tan\varphi} = k\gamma Z \\ 2\int_0^{x_0}\tau_{xz}dx + mAk\gamma Z - P = 0 \end{cases}. \tag{32}$$

With the above derivation:

$$\int_0^{x_0}\tau_{xz}dx = \frac{B_0 mA}{2}\left(1 - e^{\frac{2\tan\varphi}{mA}x_0}\right) \tag{33}$$

$$\begin{cases} B_0 e^{\frac{2\tan\varphi}{mA}x_0} - \dfrac{C}{\tan\varphi} = k\gamma Z \\ mAB_0(1 - e^{\frac{2\tan\varphi}{mA}x_0}) + Ak\gamma Zm - P = 0 \end{cases}. \tag{34}$$

It can be solved that

$$B_0 = \frac{C}{\tan\varphi} + \frac{P}{mA}. \tag{35}$$

Inserting Eqs. (35) and (31) into Eq. (30):

$$\sigma_z = \left(\frac{C}{\tan\varphi} + \frac{P}{mA}\right)e^{\frac{2\tan\varphi}{mA}x_0} - \frac{C}{\tan\varphi} = K\gamma Z. \tag{36}$$

To sum up, the yield zone width in a balanced stress state is

$$x_0 = \frac{mA}{2\tan\varphi}\ln\left(\frac{k\gamma Z + \frac{C}{\tan\varphi}}{\frac{C}{\tan\varphi} + \frac{P}{mA}}\right). \tag{37}$$

Application and example

Prediction method for surface residual subsidence of low-carbon gasification coal mining

The steps to predict the surface residual subsidence and deformation extreme value in the mining area of a single short working face are as follows:

(1) Employing the probability integral method (PIM) to predict the surface subsidence and deformation values before yielding and stripping of the coal walls on both sides of the combustion space area.

(2) Calculation of the sum of maximum stripping and yielding width of the coal pillar based on the proposed model.

(3) Using the PIM to predict the surface subsidence and deformation values after yielding and stripping of coal walls.

(4) The predicted surface subsidence and deformation values before and after yielding and stripping of the "hyperbolic" coal pillar are compared to obtain the surface residual deformation of UCG, and then the residual deformation prediction of the surface of the gasification site is realized.

Overview of the study area

The UCG area in the Ulanqab Mine is located in the central part of Inner Mongolia Autonomous Region, China, which is owned by Xin'ao Gasification Coal Mining Technology Co. As shown in Fig. 7, the terrain in this area is flat, with the

convenient transportation. The area where the working face is located is mostly covered by the Quaternary, and a small amount of Tertiary basalt is exposed in the western part of the mining area. The $2^{\#}$ coal seam is a gasification coal seam, with a depth of $273 \sim 278.5$ m, and the average burial depth is 275.75 m. In addition, the thickness of the coal seam is 5 m, the width of the coal pillar is 24 m, and the width of the gasification working face is 16 m. The coal in this seam is mainly lignite, and its ash yield is $12.88 \sim 42.54\%$, with an average of 27.85%. The percentage of silica in coal ash is the highest, and the general proportion is $2.96 \sim 62.48\%$, with an average proportion of 49.48%.

Application and verification

To calculate the maximum stripping and yield zone width after UCG, the ash generation rate was taken as 0.2785, the stripped coal block hulking coefficient was 1.1, and the rest angle was 45° according to the actual measurement and empirical data. Taking the above data into Eqs. (2) and (11), respectively, it can be calculated that the ash height after gasification is 1.39 m and the maximum stripping width of the coal pillar is 0.91 m.

Table 1 shows the selected coefficients when using the horizontal layer analysis method to solve the ash side pressure.

Substituting into Eq. (14), the lateral pressure of ash is 26.57 kN.

This paper is based on the elastic–plastic limit theory, and the mechanical parameters of coal pillars are shown in the following table.

Substituting into Eq. (37), the maximum yield width of coal pillar is 7.03 m (Table 2).
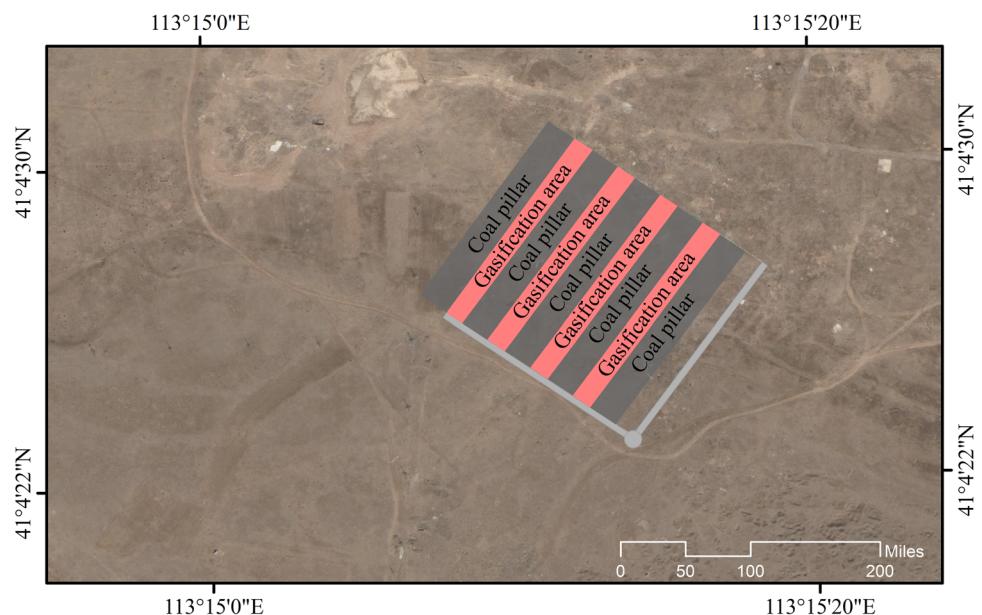
Fig. 7 Experimental area location

Table 1 Mechanical parameters between coal pillar and ash

The inclination angle of the most dangerous sliding surface (°)	Coal pillar and ash friction angle (°)	Internal friction angle of ash (°)	Angle between coal pillar and vertical plane (°)	Average gravity density (kpa/m³)
37.092	11.67	35	40.57	13

Table 2 Mechanical parameters of coal pillar

Cohesion (kpa)	Internal frictional angle (°)	Coefficient of lateral pressure	Effective unit weight (kpa/m³)
80	33.28	0.4	24.5

Table 3 Predicted parameters of surface subsidence before coal pillar stripping and yielding

Subsidence coefficient	Horizontal displacement factor	Tangent of main influence angle (°)	Mining influence angle (°)	Offset distances of inflection points
0.03	0.24	1.76	89	0

Table 4 Predicted parameters of surface subsidence after coal pillar stripping and yielding

Subsidence coefficient	Horizontal displacement factor	Tangent of main influence angle (°)	Mining influence angle (°)	Offset distances of inflection points
0.031	0.24	1.76	89	0

According to the A. H. Wilson strip coal pillar stability calculation method (Wilson 1983), under the action of the overburden pressure, the edge of the coal pillar undergoes plastic deformation and generates a yield zone. Let the yielding area width be Y(m), mining depth be H(m), and mine width be w(m):

$$Y = 0.0049wH. \tag{38}$$

Considering the geological mining conditions, the calculated width of the yield zone is 6.76 m.

The calculation method of strip-mining stability has problems caused by simplification, which does not incorporate the side pressure of ash and coal pillar "hyperbolic" characteristics after UCG, so 7.03 m is selected as the width of coal pillar yield zone after UCG is safer and more reliable.

From the most unfavorable conditions, it is considered that the total width of the loss of bearing is the sum of the stripping width and yield zone width of the coal pillars on both sides of the combustion space area, that is: $7.03 + 0.91 = 7.94$ m.

From the literatures (Li et al. 2017), PIM is applicable for the surface residual subsidence of UCG. The PIM is developed and established on the basis of the stochastic medium theory, which is the most commonly used method for predicting surface subsidence estimation in the field of mining subsidence. Therefore, this paper also adopts the PIM to calculate the surface subsidence and deformation values of UCG. The predicted parameters of surface subsidence before and after UCG are summarized in Tables 3 and 4.

According to the prediction values, the surface residual subsidence contour lines, horizontal residual displacement contour lines, surface tilt contours and surface residual horizontal deformation contours of the UCG experimental area based on the PIM can be drawn. Due to the limited space, only the surface residual subsidence contours of the industrial experiments of UCG are shown in Fig. 8.
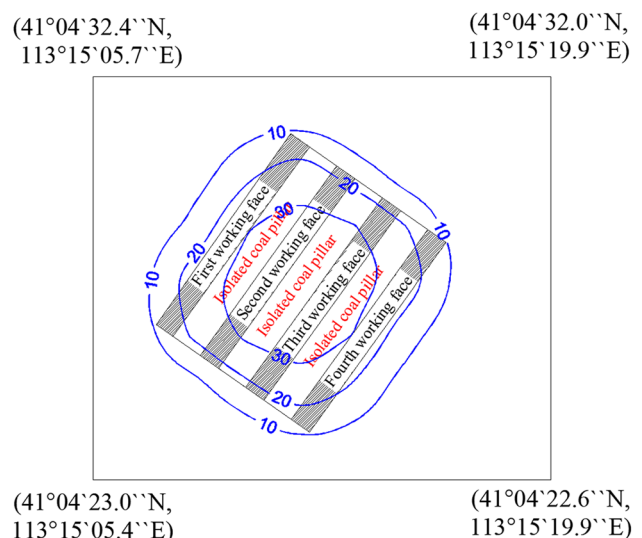

Fig. 8 Surface subsidence contour lines in the UCG experimental area based on the PIM

Only one observation points was set up in the industrial experiment of UCG in Ulanqab. Because of the small number of monitoring points, it cannot be used to learn the surface residual subsidence, but it can offer an important real measurement reference for the data comparison for the PIM of surface residual subsidence. This observation point is located in the middle of the second and third gasification working faces, 10 m away from the maximum subsidence point. According to the actual measurement, the measured subsidence value of this point is 36 mm after the UCG is completed. The maximum value of surface subsidence before stripping and yielding is calculated by the PIM to be 39 mm, which is relatively close to the measured value.

Considering that the measured point is not the maximum subsidence point, the prediction result is considered reliable, because the measured point is not the maximum sinkage point. The maximum value of surface subsidence after stripping is 74 mm, so the maximum value of surface residual subsidence of the UCG test area is 35 mm.

Conclusion

(1) The main reason for the surface residual subsidence of UCG is the stripping and yield softening of the "hyperbolic" coal pillar under the action of long-term groundwater, weathering, overburden pressure, and other factors, resulting in the increase of the arch foot and arch height of the overlying stress balance arch, which in turn causes the "secondary" deformation of the gasification site.

(2) Combined with the characteristics of coal pillars and ash accumulation after UCG, the calculation model of the maximum stripping width of "hyperbolic" isolated coal pillars after UCG was established by theoretical analysis method. In addition, an elastic–plastic limit theory was used to derive a model for calculating the maximum yield zone width of the "hyperbolic" coal pillar after UCG, which provides a theoretical basis for the prediction of the surface residual subsidence of the UCG.

(3) The method for predicting the residual subsidence on the surface of UCG that considers the stripping and yielding of "hyperbolic" coal pillars is proposed, which solves the problem of predicting the residual deformation on the surface of UCG and is applied to the UCG test area in Ulanqab. It can be concluded that the maximum subsidence value of the surface residual deformation in the gasification test area is 35mm.

Author contributions Conceptualization: CT and HL; methodology: CT and HL; validation: WL and FC; formal analysis: XZ; investigation: CL and GD; data curation: YY; writing–original draft preparation: HL and CT; writing–review and editing: HL and CT; visualization: XZ; supervision: GG and JZ; project administration: GG and JZ; funding acquisition: HL. All authors reviewed the manuscript.

Declarations

Conflict of interest The authors declare no conflict of interest.

References

Al-Ghussain L (2019) Global warming: review on driving forces and mitigation. Environ Prog Sustainable Energy 38(1):13–21

Ariyoshi D, Takeda S, Kosuge K, Mizuno M, Kato K (2016) Development of high-efficiency coal gasification technology. Springer, Singapore, pp 617–619

Bhutto AW, Bazmi AA, Zahedi G (2013) Underground coal gasification: from fundamentals to applications. Prog Energy Combust Sci 39(1):189–214

Chen D, Chen H, Zhang W, Cao C, Zhu K, Yuan X, Du Y (2020) Characteristics of the residual surface deformation of multiple abandoned mined-out areas based on a field investigation and SBAS-InSAR: a case study in Jilin China. Remote Sensing 12(22):3752

Cui X, Zhao Y, Wang G, Zhang B, Li C (2020) Calculation of residual surface subsidence above abandoned longwall coal mining. Sustainability 12(4):1528

Deficiency:assuming that the void will be absoluted compressed and some calculating Eq can be optimized. Journal of Cleaner Production 279.

Friedmann SJ, Upadhye R, Kong FM (2008) Prospects for underground coal gasification in carbon-constrained, 9th International Conference on Greenhouse Gas Control Technologies. Washington, DC. Energy Proc. 1:4551–4557

Guang-li G, Ka-zhong D, Zhi-xiang T, Feng-chun L (2002) Study on the prediction method of ground residual subsidence in the deep abandoned longwall goaf and its application. J Liaoning Tech Univ (natural Science) 01:1–3

Guo QB, Meng XR, Li YM, Lv X, Liu C (2021) A prediction model for the surface residual subsidence in an abandoned goaf for sustainable development of resource-exhausted cities. Deficiency:assuming that the void will be absoluted compressed and some calculating Eq can be optimized. J Clean Prod. https://doi.org/10.1016/j.jclepro.2020.123803

Hargroves K, Desha C, von Weisaecker E (2016) Introducing carbon structural adjustment: energy productivity and decarbonization of the global economy. Wiley Interdiscip Rev-Energy Environ 5(1):57–67

Huang CF, Li Q, Tian SG (2020) Research on prediction of residual deformation in goaf of steeply inclined extra-thick coal seam. PLoS ONE 15(10):e0240428

Jian Y, Yu-feng G, Yong-feng C, Xian-long L (2009) Passive earth pressure of inclined retaining walls under seismic condition. Chin J Geotech Eng 31(09):1391–1397

Johnstone P, Rogge KS, Kivimaa P, Fratini CF, Primmer E (2021) Exploring the re-emergence of industrial policy: Perceptions regarding low-carbon energy transitions in Germany, the United Kingdom and Denmark. Energy Res Soc Sci 74:101889

Ka-zhong D, Zhi-xiang T, Hong-zhen Z, Hong-dong F, Li-ya Z (2012) Research on calculating method of residual subsidence of longwall goaf. J China Coal Soc 37(0253–9993):1601–1605

Le Quéré C, Capstick S, Corner A, Cutting D, Johnson M, Minns A, Schroeder H, Walker-Springett K, Whitmarsh L, Wood R (2015) Towards a culture of low-carbon research for the 21st Century. University of East Anglia, Tyndall Centre

Li HZ, Guo GL, Zha JF, He Y, Wang ZY, Qin SY (2017) Stability evaluation method for hyperbolic coal pillars under the coupling effects of high temperature and ground stress. Environ Earth Sci. https://doi.org/10.1007/s12665-017-7048-0

Li PX, Yan LL, Yao DH (2019) Study of tunnel damage caused by underground mining deformation: calculation, analysis, and reinforcement. Adv Civil Eng. https://doi.org/10.1155/2019/4865161

Luan YZ, Dong Y, Ma Y, Weng L (2020) Surface and new building deformation analysis of deep well strip mining. Adv Mater Sci Eng 2020:8727956. https://doi.org/10.1155/2020/8727956

Prabu V (2015) Integration of in-situ CO2-oxy coal gasification with advanced power generating systems performing in a chemical looping approach of clean combustion. Appl Energy 140:1–13

Qin L, Kirikkaleli D, Hou Y, Miao X, Tufail M (2021) Carbon neutrality target for G7 economies: examining the role of environmental policy, green innovation and composite risk index. J Environ Manag 295:113119

Salamon BJ, Madden MU (1998) Life and design of bord-and-pillar workings affected by pillar scaling. J South Afr Inst Min Metall 98(3):135–145

Slamersak A, Kallis G, O'Neill DW (2022) Energy requirements and carbon emissions for a low-carbon energy transition. Nat Commun. https://doi.org/10.1038/s41467-022-33976-5

Sovacool BK (2022) A perspective on treaties, maximum wages, and carbon currencies: innovative policy instruments for global decarbonization. Energy Policy 160:112702

Suzuki M, Kanie N, Iguchi M (2016) New approaches for transitions to low fossil carbon societies: promoting opportunities for effective development, diffusion and implementation of technologies, policies and strategies. J Clean Prod 128:1–5

Van der Merwe JN (2003) Predicting coal pillar life in South Africa. J S Afr Inst Min Metall 103(5):293–301

van der Merwe JN, Mathey M (2013) Update of coal pillar database for South African coal mining. J South Afr Inst Min Metall 113(11):825–840

Walker LK (2014) Underground coal gasification: issues in commercialisation. Proc Inst Civ Eng Energy 167(4):188–195

Wilson AH (1983) The stability of underground workings in the soft rocks of the coal measures. Int J Min Eng 1(2):91–187

Wu XF, Xu YC, Lou YT, Chen Y (2018) Low carbon transition in a distributed energy system regulated by localized energy markets. Energy Policy 122:474–485

Xie J, Xin L, Hu XM, Cheng WM, Liu WT, Wang ZG (2020) Technical application of safety and cleaner production technology by underground coal gasification in China. J Clean Prod 250:119487

Yang Y, Kazhong D, Hongdong F (2017) Long-term stability evaluation and coal pillar design methods for strip mining. J China Coal Soc 42(12):3089–3095

Yu Y, Deng KZ, Luo Y, Chen SE, Zhuang HF (2018) An improved method for long-term stability evaluation of strip mining and pillar design. Int J Rock Mech Min 107:25–30

Zheng M, Deng K, Fan H, Du S (2018) Monitoring and analysis of surface deformation in mining area based on InSAR and GRACE. Remote Sens 10(9):1392

Zheng M et al (2018) Monitoring and analysis of surface deformation in mining area based on InSAR and GRACE. Remote Sens 10(9):1392